Experimental and Numerical Investigation of Rotating Stall Phenomenon in Centrifugal Blower at Different Blade Number of the Impeller

Asst. Prof. Dr. Muna Sabah Kassim
Mechanical Department, College of Engineering, Al-Mustansiriyah University
www.munahdr@yahoo.com

Asst. Prof. Dr. Foad Aluan Saleh
Mechanical Department, College of Engineering, Al-Mustansiriyah University
www.foads2003@yahoo.com

Mohammed Abdalnabee Kadhum
Mechanical Department, College of Engineering, Al-Mustansiriyah University
www.mohammedabdalnabee@yahoo.com

Abstract

Experimental and numerical investigations to study the effect number of blade on the rotating stall phenomenon and pressure fluctuations in centrifugal blower. The experimental test rig which concludes a centrifugal blower, pressure sensors and measurement instrumentations are design and constructed for the present work. A data acquisition system (hardware) and its software have been designed and manufactured to transfer the signal from pressure sensor to the computer and then analysis with time and frequency domain.

The experimental study has been carried out by measuring the static pressure variation and pressure fluctuation for three cases of impeller which they different in number of blades (5, 9, 10) and outlet blade angle. Measuring of static values has been completed at various points prepared on the front-wall of the volute casing along one path for three cases of impeller. This path is angular path around the impeller.

The experimental results demonstrate that the pressure fluctuations for various mass flow rates are a non-periodical nature and the pressure fluctuations amplitude increase as the mass flow rate decrease. The results indicate that the impeller with nine number of blades demonstrate high pressure fluctuation comparison with other case.

Numerical simulation has been carried out on present centrifugal blower to analyze both flow field and pressure fluctuations by using FLUENT 14 package. The numerical simulation has been completed by solving the continuity and momentum equations with moving reference frame technique inside the blower. A comparison of pressure fluctuations inside the blower with various numbers of blades was carried out. The results of numerical simulation give a good agreement with the experimental results.

Keywords: rotating stall, centrifugal blower, impeller.

تحري عملي وعددي لظاهرة الانهيار الدوار في نافخ طارد مركزي لعدد مختلف لريش البشارة

ا.م.د منى صباح قاسم ا.م.د فؤاد علوان صالح محمد عبدالنبي كاظم
قسم الهندسة الميكانيكية / الجامعة المستنصرية

الخلاصة

في هذا العمل تم انجاز دراسة عملية ونظرية لدراسة تاثير عدد ريش الدافعة على ظاهرة الانهيار الدوار وتذبذب الضغط في نافخ هواء مركزي. الدراسة تمت باستخدام متحسس الضغط ومعدات قياس الجريان التي صممت لتناسب متطلبات هذا البحث. كما تم تصميم وتصنيع معالج الاشاره لنقل الاشاره من متحسس الضغط الى جهاز الكمبيوتر ليتم تحليلها بدلالة الزمن والتردد. الدراسة التجريبية نفذت بقياس التغير الحاصل في الضغط وتذبذب الضغط لثلاث حالات للدافعة تختلف في عدد الريش (10,9,5) وزاوية الريشة. تمت قراءة قيم الضغط لعدة نقاط والتي اعدت خصيصا على الجدار الامامي للمجمع ولمسار واحد هو مسار محيطي حول الدافعة.

النتائج العملية اظهرت الطبيعة غير المتزامنة لتذبذب الضغط لمختلف معدلات الجريان بالاضافة الى ان تذبذب الضغط يرتفع عند نقصان معدلات الجريان. كما اظهرت النتائج العملية بان الدافعة مع عدد ريش (9) تظهر معدلات تذبذب للضغط عالية مقارنة بالحالات الاخرى للدافعة.

محاكاة عددية تم انجازها لنافخ الهواء لتحليل جريان المائع وتذبذب الضغط باستخدام برنامج FLUENT 14. المحاكاة العددية تمت بحل معادلات الاستمرارية والزخم مع تقنية الهيكل الدوار للنافخ. مقارنة تذبذب الضغط داخل النافخ المركزي مع عدد ريش مختلفة ولمختلف معدلات الجريان تم اجرائها. نتائج المحاكاة العددية للجريان قدمت نتائج متوافقة وبصوره جيده مع نتائج التجارب العملية.

Nomenclature

D	Impeller exit diameter (m)
d	Impeller inlet diameter (m)
Z	Number of blade
β	Blade angle (deg)
ΔP	Pressure difference (pascal)
r	Radius (m)
$\dot{m}$	Mass flow rate (kg/s)
C	Discharge coefficient
Re	Reynolds number
$\emptyset$	Circumferential angle (deg)
SST	Shear stress transform
u, v, w	Velocity component (m/s)

1. Introduction

Compressors , turbines and fans are all members of the same family of machines called turbo machines . A turbo machine is a power or head generating machine which employs the dynamic action of a rotating element (i.e. the rotor) the action of the rotor changes the energy level of the continuously flowing fluid through the turbo machine [1].

Stability is a very important factor and one of the main concerns of blower designers and users. When flow rate reduces, blowers have a limited stable operating range, due to the occurrence of unsteady phenomenon like rotating stall or surge. Rotating stall is a two-dimensional, local instability phenomenon in which one more local regions of stagnant flow, so-called stall cells, rotate around the circumference of the blower [2]. Surge is characterized by large amplitude fluctuations of the pressure and unsteady, but circumferentially uniform, annulus-averaged mass flow [3]. This is essentially one-dimensional instability; it affects the compression system as a whole and results in a limited cycle oscillation in the blower map. These instabilities can lead to severe damage of the machine because of large mechanical and thermal loads in the blading, and consequently restrict its performance and efficiency [4].

A great deal of work has been carried out on flow behavior investigation in various parts of the turbo machines, e.g. inlet duct, impeller, vane and vane less diffuser, volute, and outlet duct, etc. Imaichi et al. [5] carried out test on a centrifugal fan to study the rotating stall cells in the fan. The main results from this work show that the rotating stall cells travel only in the direction of the impeller rotation, and at lower flow rates, there are two rotating cells. Hamada et al. [6] investigated the flow patterns around three volute tongue designs, volute A, a full tongue was used, volute C, the tongue was cut back. The third design the leading edge of the tongue was rounded. By cutting back the volute tongue both the volute and fan performance was improved. The performance was then further improved by providing a rounded leading edge to the volute tongue. Zhou et al. [7] described a three-dimensional simulation of internal flow in three different centrifugal pumps using the CFD, and their comparison of numerical results for various types of pumps showed good agreement for twisted-blade pumps, but not for straight-blade one. Eduardo et al. [8] analyzed an experimental and numerical study on the unsteady flow through a single suction and single volute centrifugal pump equipped with four impellers of different outlet diameter. The results indicate that the unsteady phenomena at the blade passage frequency clearly depend on the value of the impeller-tongue gap. Saad [9] investigated the feasibility of controlling the stall in radial diffuser of a low speed centrifugal blower using a very simple technique that involved using rough surfaces attached to the diffuser (stall) was delayed to a lower flow coefficient (the mass flow rate could be reduced to 70% of its value with a smooth surface) when the rough surfaces were position on the diffuser

walls. Stefan [10] investigated the flow instabilities and rotating stall in a high-energy centrifugal pump stage. The measurements in the impeller trailing edge allowed the identification of stall in different diffuser channels, which were observed as rotating or stationary discontinuities in the periodic pressure fluctuation patterns. He show that the rotational speed of the stall cells was less than 1% of the impeller rotational speed.

In this work, experimental and numerical investigations have been applied in order to obtain the pressure fluctuations at the impeller-volute of an industrial centrifugal blower. In this work, we shall discuss the influence number of blade of impeller on rotating stall and pressure fluctuation inside the blower. The numerical results have been compared with experimental results obtain from pressure transducer which install on the casing of blower. The aim from the present work to provide a complete description of the flow field within the blower and to evaluate the capabilities of the numerical model to describe the unsteady flow features in the blower.

2. Description of the Blower and Experimental Procedures.

The tested machine is a centrifugal blower driven by an AC 600W motor which has rotational speed 16000 rpm. The unshrouded impellers tested have (5, 9, 10) backward-curved blades with an outlet diameter of 110mm. The distance between the impeller and the volute tongue is (12 mm). **Table (1)** and **Figure (1)** summarizes the main dimensions of its impeller.

The test rig, as shown in the **Figure (2),** has been designed and constructed to be appropriate for the purpose of the present and future research. The test rig has been constructs to form an open loop system. The loop consisted of a constant-speed electric blower, a throttle valve, a metering orifice, and piping. The air is collected by a scroll (volute) of circular cross sectional area. The outlet pipe of the blower is connected to an orifice plate air flow meter through (90 mm) length flexible pipe. The throttle valve (gate valve), fitted on the discharge side of the piping, and allows an accurate and fine control of the mass flow rate.

The static pressure measurements are carried out, by employing a strain gauge pressure transducer. The transducer is designed in order to indicate a differential pressure. The output signals from the transducer are appropriately conditioned and digitized using the data acquisition system. The output signals are also connected to an oscilloscope, to monitor the onset of any perturbation in the flow. This observation will give a continuous display of the variation and measurement problems in order to avoid it.

The measurement for the present study is carried out on the front-wall of the casing. Several measurement taps are arranged on this wall, as shown in Figure (3). The numbers of these taps are twelve and located at every 30^0 interval around the front side of the impeller, and at location of 5mm from the outlet of the impeller.

Table .(1) Main Characteristics of the Tested Impeller

Impeller parameters	Case A	Case B	Case C
Impeller exit diameter	D =110 mm	D =110 mm	D =110 mm
Impeller inlet diameter	d =28 mm	d =28 mm	d =28 mm
Number of impeller blade	Z = 10	Z = 9	Z = 5
Rotational speed	16000 rpm	16000 rpm	16000 rpm
Inlet blade angle	$\beta_1 = 54^\circ$ from tangential direction.	$\beta_1 = 54^\circ$ from tangential direction.	$\beta_1 = 54^\circ$ from tangential direction.
Outlet blade angle	$\beta_2 = 42^\circ$ from tangential direction.	$\beta_2 = 48^\circ$ from tangential direction.	$\beta_2 = 42^\circ$ from tangential direction.
Blade thickness	3 mm	3 mm	3 mm

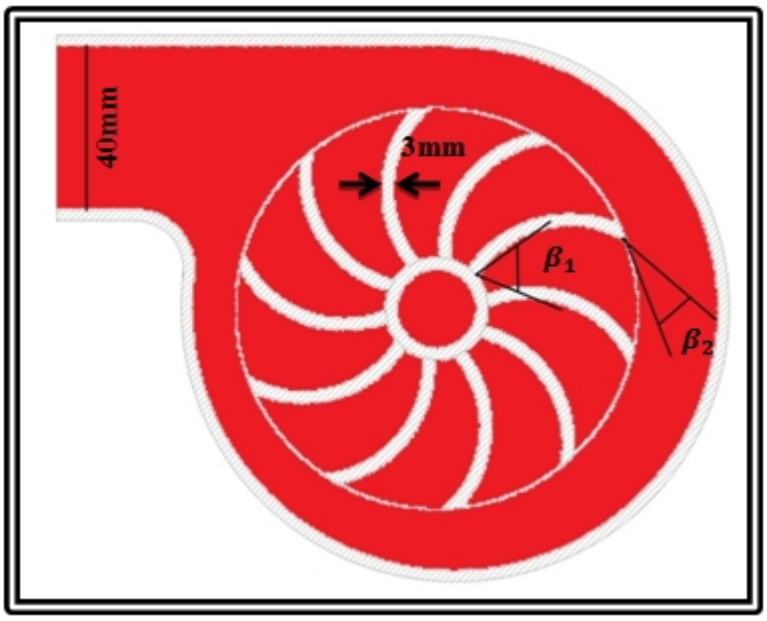

Fig .(1) Impeller View and Cross-Sectional View of the Centrifugal Blower

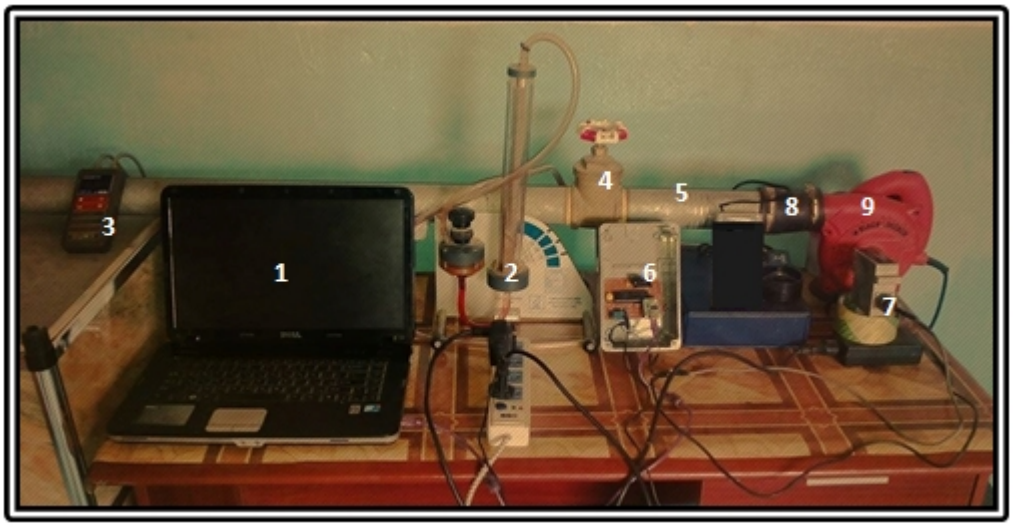

1- Personal computer 2- U-Tube manometer 3- Digital manometer
4- Gate Valve 5- Pipe 6- interface card (ADC)
7- Transducer 8- Flexible pipe 9- Centrifugal blower

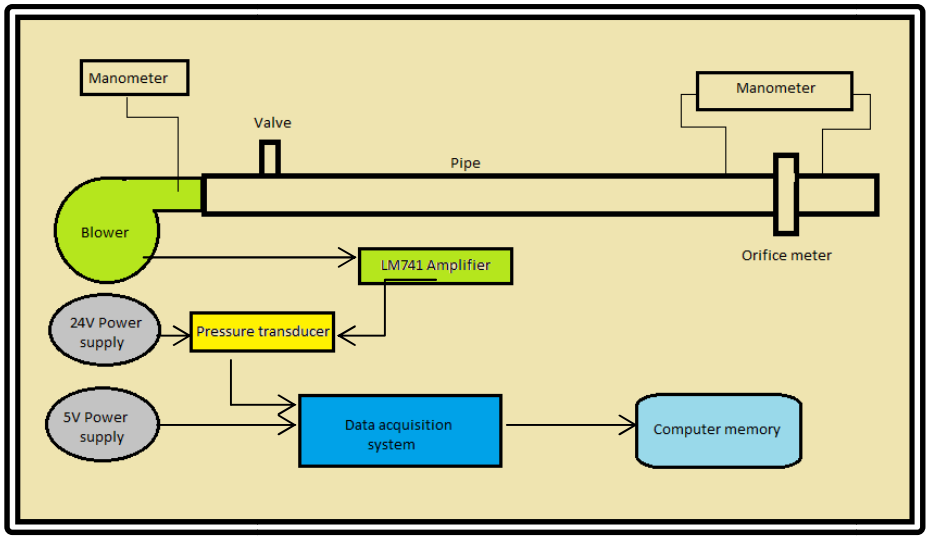

Fig .(2): Test Rig

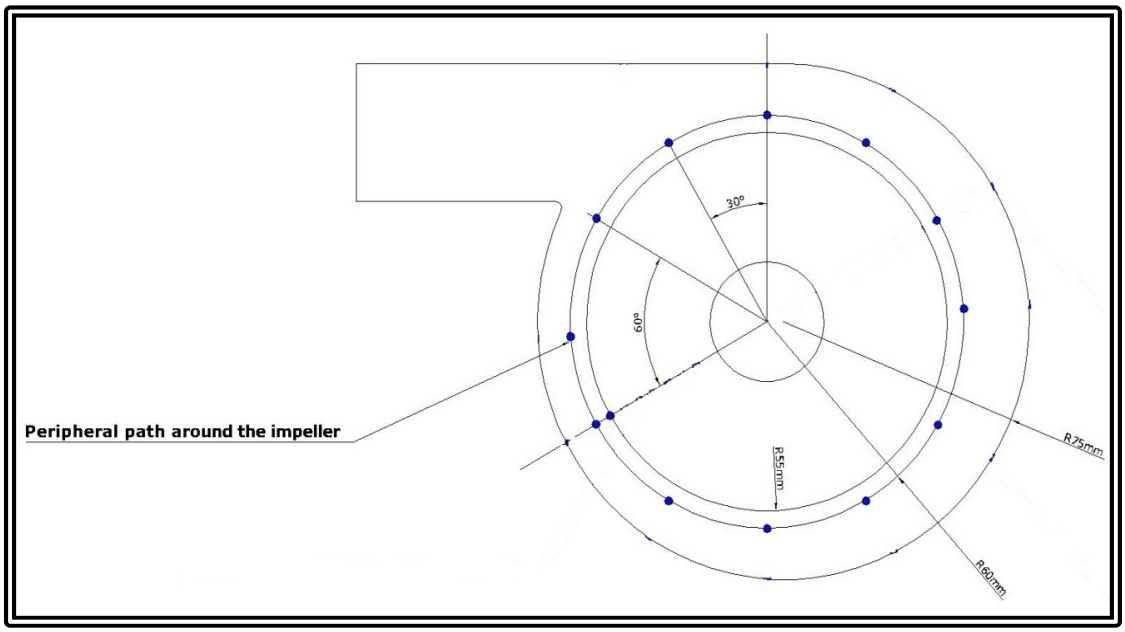

Fig .(3) Locations of Measuring Points

3. Numerical Flow Simulation

In parallel with the measurements, numerical simulations of the unsteady flow in the centrifugal blower described above were carried out. In order to verify the capabilities of the numerical model to describe the flow features inside the blower, a three-dimensional numerical simulation of the unsteady flow has been carried out. All the calculations have been performed with commercial software package **FLUENT 14**. This code uses the finite volume method and Navier-Stokes equations.

The conservation equation for continuity and momentum equations can be written as follows [11]:

- **Continuity equation**

$$\frac{\partial \bar{u}}{\partial x} + \frac{\partial \bar{v}}{\partial y} + \frac{\partial \bar{w}}{\partial z} = 0 \qquad \text{..... (1)}$$

- **Momentum equation in x-direction**

$$\left(\bar{u}\frac{\partial \bar{u}}{\partial x} + \bar{v}\frac{\partial \bar{u}}{\partial y} + \bar{w}\frac{\partial \bar{u}}{\partial z}\right) = -\frac{1}{\rho}\frac{\partial P}{\partial x} + \nu\nabla^2\bar{u} + \left(-\frac{\partial}{\partial x}\left(\overline{\acute{u}^2}\right) - \frac{\partial}{\partial y}\left(\overline{\acute{u}\acute{v}}\right) - \frac{\partial}{\partial z}\left(\overline{\acute{u}\acute{w}}\right)\right)$$

..... (2)

- **Momentum equation in y-direction**

$$\left(\bar{u}\frac{\partial \bar{v}}{\partial x}+\bar{v}\frac{\partial \bar{v}}{\partial y}+\bar{w}\frac{\partial \bar{v}}{\partial z}\right)=-\frac{1}{\rho}\frac{\partial P}{\partial y}+\nu\nabla^2\bar{v}+\left(-\frac{\partial}{\partial y}\left(\overline{\acute{v}^2}\right)-\frac{\partial}{\partial x}\left(\overline{\acute{u}\acute{v}}\right)-\frac{\partial}{\partial z}\left(\overline{\acute{v}\acute{w}}\right)\right)$$

…….. (3)

- **Momentum equation in z-direction**

$$\left(\bar{u}\frac{\partial \bar{w}}{\partial x}+\bar{v}\frac{\partial \bar{w}}{\partial y}+\bar{w}\frac{\partial \bar{w}}{\partial z}\right)=-\frac{1}{\rho}\frac{\partial P}{\partial z}+\nu\nabla^2\bar{w}+\left(-\frac{\partial}{\partial z}\left(\overline{\acute{w}^2}\right)-\frac{\partial}{\partial x}\left(\overline{\acute{u}\acute{w}}\right)-\frac{\partial}{\partial y}\left(\overline{\acute{v}\acute{w}}\right)\right)$$

…….. (4)

In the present work, the following assumptions were taken for simulation:

1- The walls of the casing were assumed to be smooth hence any disturbances in flow due to roughness of the surface were neglected.
2- The friction coefficients for all surfaces were set to, hence friction between the walls and fluid was neglected.
3- Steady state conditions, incompressible fluid flow, turbulent flow and Newtonian fluid.
4- Three dimensional flow simulations.

Geometrical discretization of the centrifugal blower is made for the numeric treatment, and computational grid is generated using ***FLUENT*** preprocessor ***Gambit***. There are mainly two types of approaches in volume meshing, structured and unstructured meshing. In structured mesh, the governing equations are transformed into the curvilinear coordinate system aligned with the surface. However; it becomes extremely inefficient and consumes time for complex geometries. Therefore, it has been excluded in this research. In the unstructured approach, the integral form of governing equations is discretized and either a finite-volume or finite-element scheme is used. Unstructured grids are in general successful for complex geometries, so it was used in present work. **Figure (4),** shows the mesh of centrifugal blower. The final point in a good mesh is the total number of cells generated. It is vital to have enough number of cells for a good resolution but memory requirements increase as the number of cells increase. In this study the average number of mesh are (3400000 cells).

A control-volume based technique that consists of the following steps is used for solution [12]:

1- For velocity, pressure, and conserved scalars, algebraic sets of equations are constructed by the integration of the governing equations on each control volume.
2- Discretized equations are linearized and solved iteratively.

The modeled boundary conditions are those considered with more physical meaning for turbomachinary flow simulations, that is, total pressure at the domain inlet and static pressure proportional to the kinetic energy at the domain outlet[13]. The flow rate is changed by modifying the pressure at the outlet condition, which simulates the closure of a valve. Turbulence is simulated with SST, $\mathcal{K}$-ω model. The semi-implicit method pressure link equation (SIMPLE) algorithm, second order, upwind discretization have been used to perform the solution of flow inside the blower.

Fig .(4) The Mesh of Centrifugal Blower Generated in the Gambit

4. Results and Discussions

In this section, we shall discuss the results related to the behavior of the flow in impeller-volute of a centrifugal blower. In this work a detailed study and analysis of the rotating stall in term of pressure fluctuations in time and frequency domains has carried out. The experimental were carried out under constant speed (16000 rpm) and variable mass flow rates. The pressure fluctuations take at one point on the casing of centrifugal blower. This point at the exit of impeller ($r/r_i = 1$) and at angular position 60°. **Tables (2), (3) and (4)** show the details of calculations of the mass flow rates. The values were chosen arbitrarily but the maximum values of the mass flow were limited by the control valve design and rotational speed.

Table .(2) Details of Final Calculation for Mass Flow Rate (Case A).

ΔP (pas)	Rotational speed (rpm)	$R_{eD}\times10^3$	C	ṁ (k_g/s)
0	16000	0	0	0
1970	16000	18.838	0.6070	0.01607
3890	16000	26.423	0.6059	0.02254
5640	16000	31.792	0.6055	0.02712

Table .(3) Details of Final Calculation for Mass Flow Rate (Case B).

ΔP (pas)	Rotational speed (rpm)	$R_{eD}\times10^3$	C	ṁ (k_g/s)
0	16000	0	0	0
1810	16000	18.053	0.6072	0.01540
3710	16000	25.813	0.6060	0.02201
5530	16000	31.476	0.6055	0.02685

Table .(4) Details of Final Calculation for Mass Flow Rate (Case C).

ΔP (pas)	Rotational speed (rpm)	$R_{eD}\times10^3$	C	ṁ (k_g/s)
0	16000	0	0	0
1740	16000	17.701	0.6072	0.01510
3530	16000	25.169	0.6061	0.02147
5210	16000	30.561	0.6056	0.02607

4.1 Time and Frequency Domain Analysis

Static pressure fluctuations in time domain over a period of 3 second for various mass flow rates at angular position $\emptyset = 60^{\circ}$ and at radius ratio r/r_i = 1 around the impeller for three cases are investigated. The figures indicate that pressure fluctuations for various mass flow rates are non-periodical in nature. This result agrees with that result obtained by Ahmed Abd Ali [14].

Figure (5) shows the pressure fluctuations for various mass flow rates at rotational speed 16000 rpm for case (A). It is clear from this figure that as the mass flow rate is reduced, the pressure fluctuations amplitude increases. The maximum pressure fluctuations amplitude occurs at mass flow rate equal to nearly non-flow.

Figure (6) shows the pressure signals for various mass flow rates at rotational speed 16000 rpm for case (B). From this figure observed very high pressure amplitude at nearly non-flow and at values of mass flow rates less than 0.02201 kg/s . This observation is due to occurrence of the rotating stall.

Figure (7) shows the pressure fluctuations for various mass flow rates at rotational speed 16000 rpm for case (C). This figure indicate that the maximum pressure amplitude at nearly non-flow and at mass flow rates less than 0.01512 kg/s.

The power spectrum plots which correspond to the pressure fluctuations for various mass flow rates at angular position $\emptyset = 60^0$ for three cases are represented in **Figures (8) to (10).** The plot demonstrates the broad band component (from 0 Hz to 8 Hz) which is a manifestation of the higher level of random frequency of pressure fluctuation for various mass flow rates.

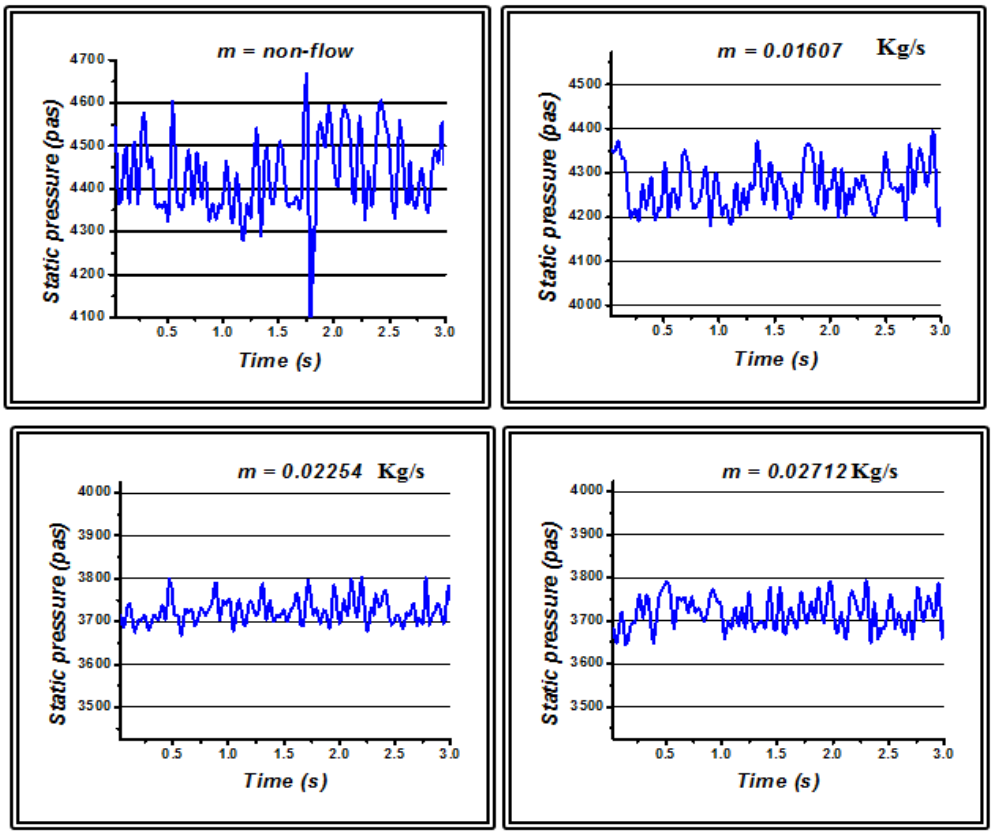

Fig .(5) Pressure Fluctuation for Various Values of Mass Flow Rates and at Rotational Speed 16000 rpm (Case A).

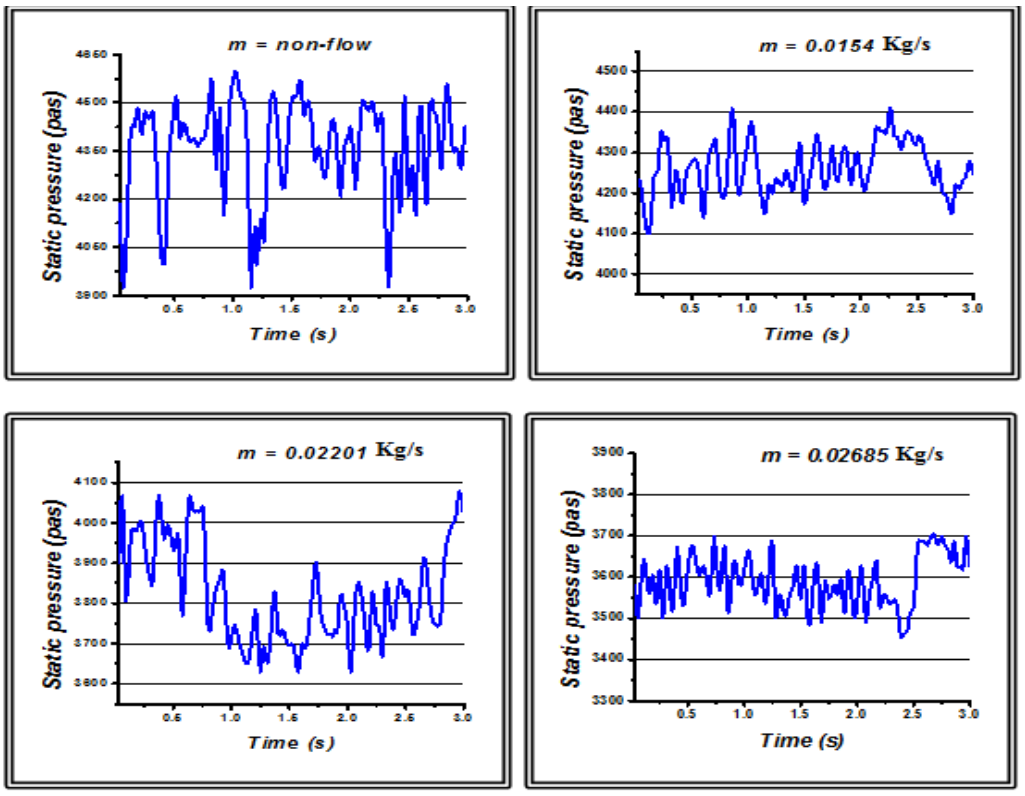

Fig .(6) Pressure Fluctuation for Various Values of Mass Flow Rate and at Rotational Speed 16000 rpm (Case B).

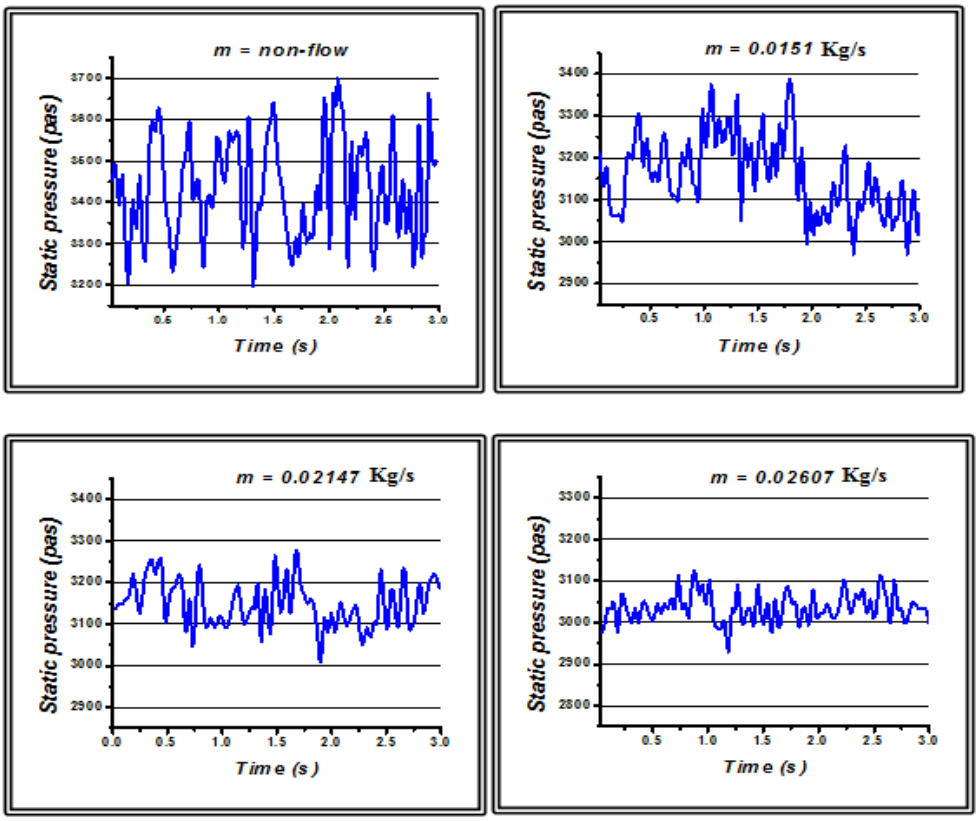

Fig .(7) Pressure Fluctuation for Various Values of Mass Flow Rate and at Rotational Speed 16000 rpm (Case C).

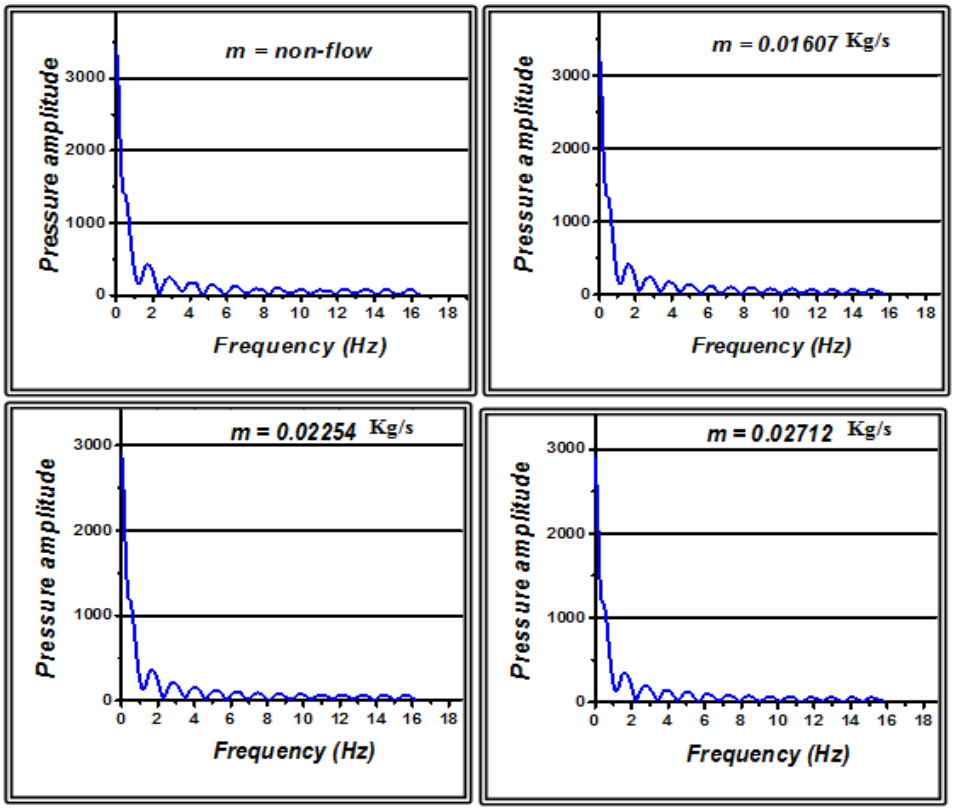

Fig .(8) Power Spectrum of Pressure Fluctuations at Various Mass Flow Rate and at Rotational Speed 16000 rpm (Case A).

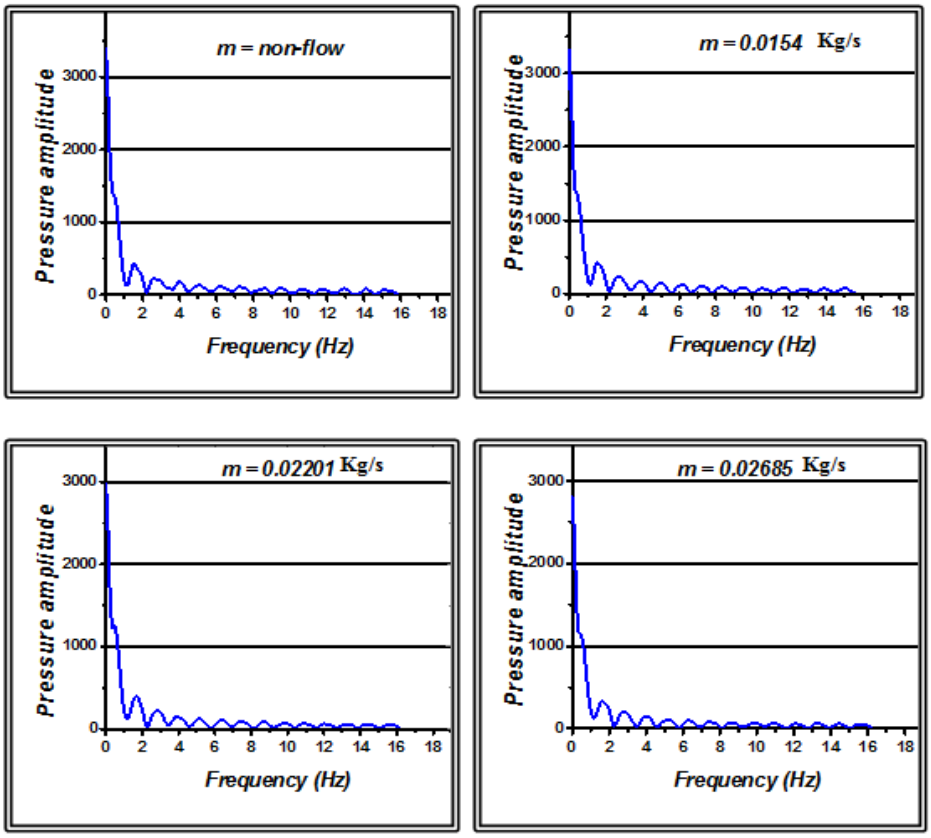

Fig .(9) Power Spectrum of Pressure Fluctuations at Various Mass Flow Rate (kg/s) and at Rotational Speed 16000 rpm (Case B).

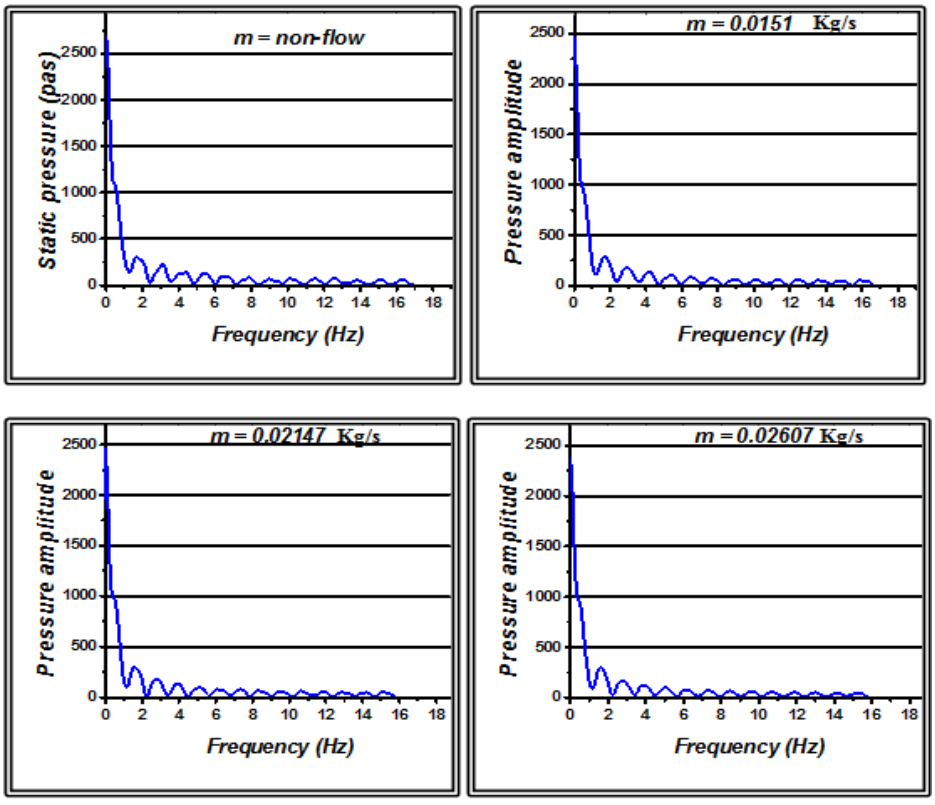

Fig .(10) Power Spectrum of Pressure Fluctuations at Various Mass Flow Rate and at Rotational Speed 16000 rpm (Case C).

4.2 Static Pressure Distribution around the Impeller

Figure (11), shows the static pressure distribution along the angular position around the impeller for three cases and for various values of flow rate at constant rotational speed (16000 rpm). The figure shows that the minimum value of static pressure in case A observed at angular position (Ø= 30˚) beyond the tongue at all values of mass flow rates. In case B observed that the minimum value of static pressure at angular position (Ø= 60˚). From the figure observed that the maximum drop in static pressure occur at angular position (Ø= 30˚). The figure, also shows that the static pressure have maximum values in the vicinity of the tongue at Ø= 0˚and at angular position Ø=330˚.

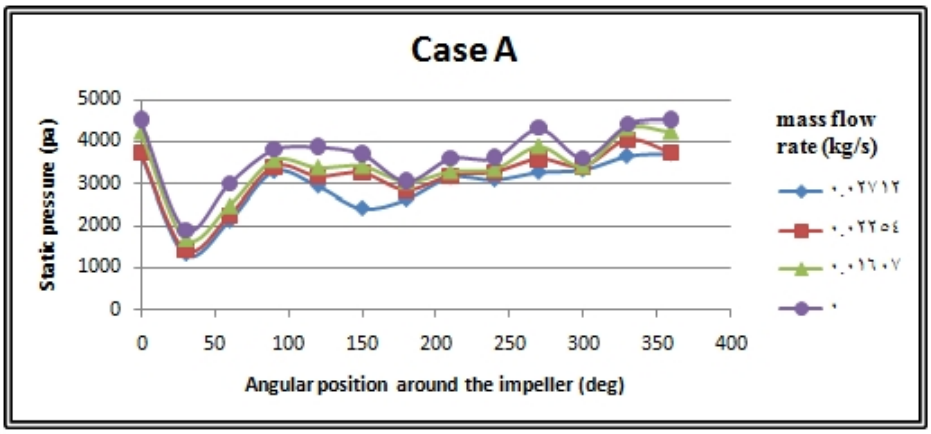

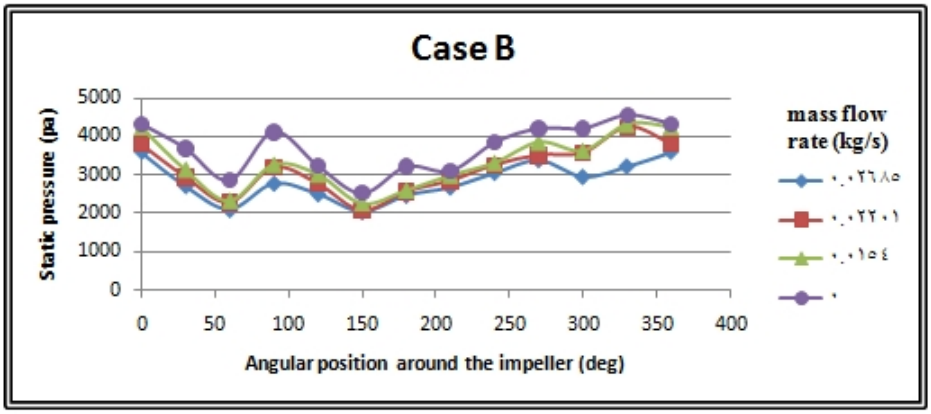

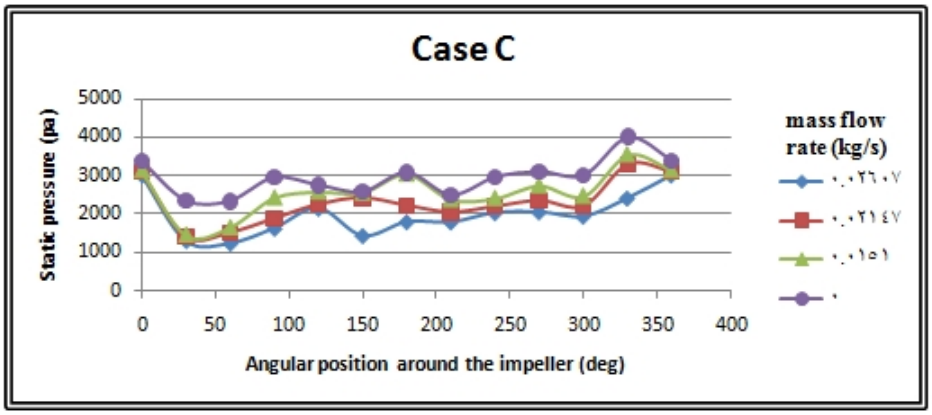

Fig .(11) Circumferential Static Pressure Distribution around the Impeller for Various Mass Flow Rate and at Rotational Speed 16000 rpm.

4.3 Analysis of Numerical Results

The possibilities of the numerical simulation in the study of the flow inside a blower are wider than the experimental ones. In particular, results corresponding to the pressure distributions inside the impeller and the flow in the volute are presented, and the unsteady calculation combined with the moving reference frame technique has proved to be a good tool to investigate the impeller-volute interaction. All the results take at the plane geometry in z-direction and at distance 21mm from the beginning of the blower casing as shown in **Figure (12).**

Figures (13) to (15) show the static pressure distribution for three cases of impeller at various mass flow rates and at rotational speed (16000 rpm). The static pressure rise through the blower is clearly seen in these figures, as are the radial pressure gradients.

The static pressure has a minimum value at the impeller eye, and around the impeller at angular position between $Ø = 60^{\circ}$ to 180° . We also observed the minimum static pressure at angular position $Ø = 300^{\circ}$. The static pressure increases between the angular position $Ø = 0^{\circ}$ to 60° and angular position $Ø = 180^{\circ}$ to $Ø = 270^{\circ}$ around the volute. The recirculation of flow observed from the distance between the tongue and the impeller exit. This lead to increase the static pressure between angular position $Ø = 0^{\circ}$ to 60°.

For cases C, observed increase the vortices and circulation of flow between the impeller blades. From this concluded that that decrease the impeller blades lead to increase pressure drop in the impeller passages.

Agreement between the numerical and experimental data is fairly good and percentage of difference between the experimental and numerical is 12%. Some differences have arisen in the comparison between the numerical and experimental static pressure in the impeller of tested centrifugal blower, especially beyond the tongue region. From this comparison it can be concluded that the increase in static pressure beyond the tongue in the numerical simulation is due to the recirculation of flow in the region between the tongue and impeller exit.

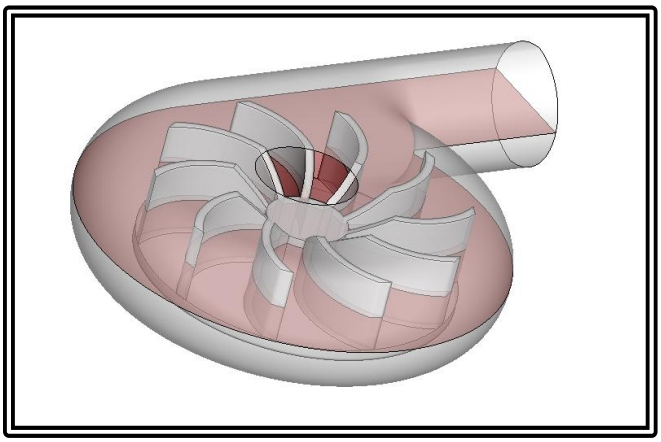

Fig .(12) plane geometry at z = 21mm

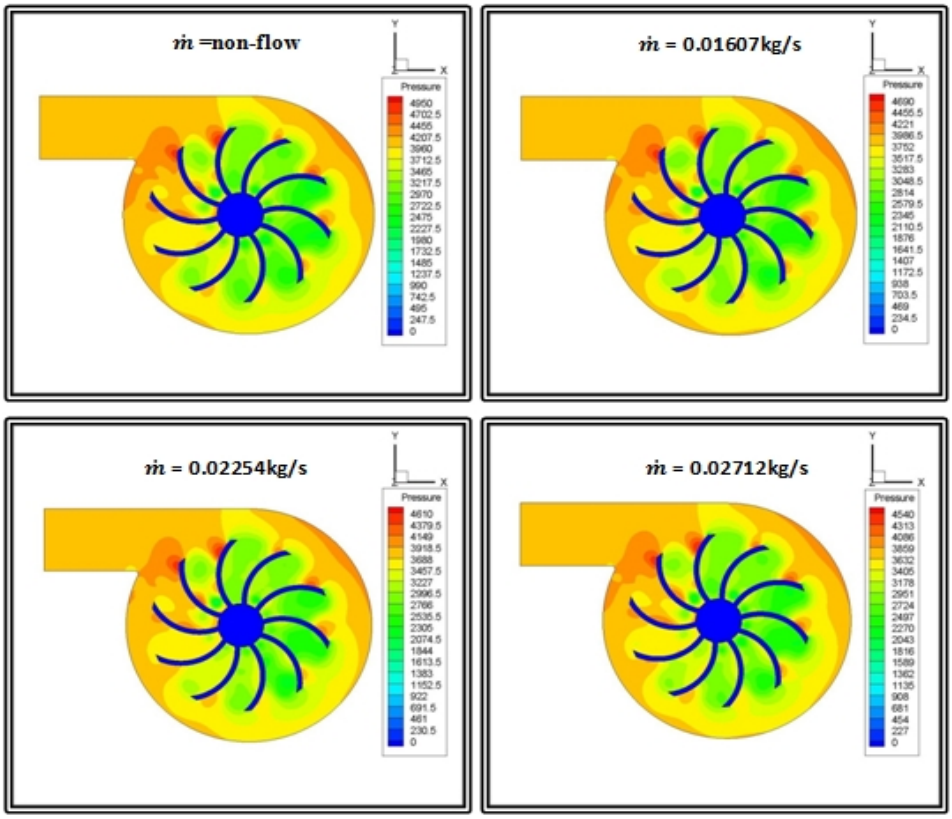

Fig .(13) Contours of Static Pressure for Case (A) at Rotational Speed 16000 rpm.

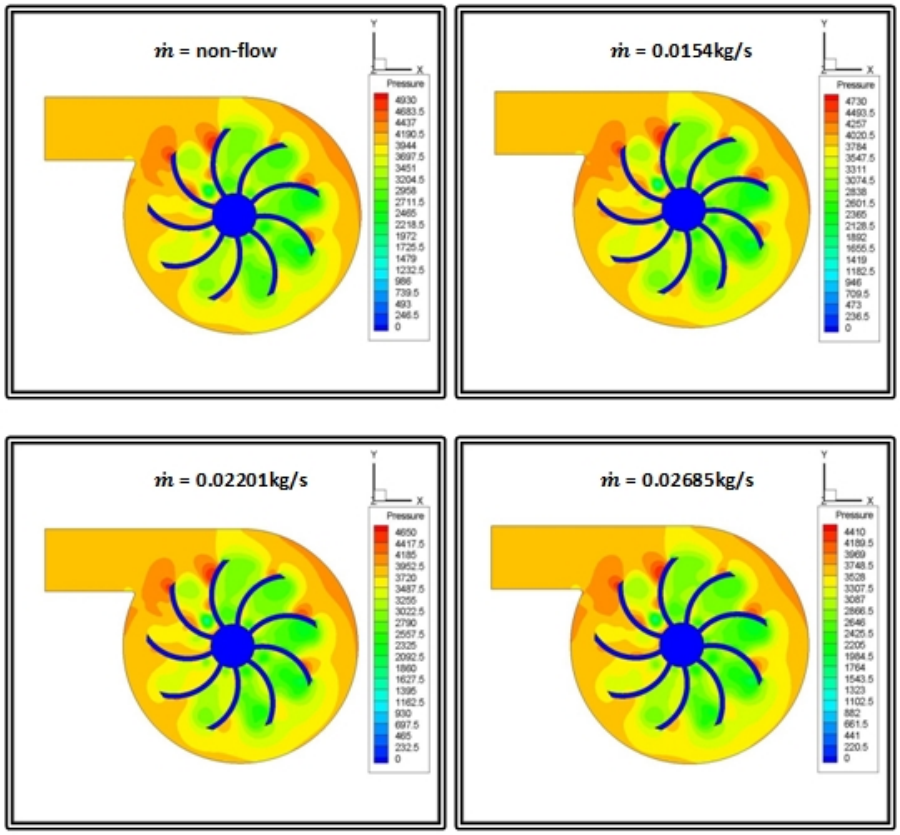

Fig .(14): Contours of Static Pressure for Case (B) at Rotational Speed 16000 rpm.

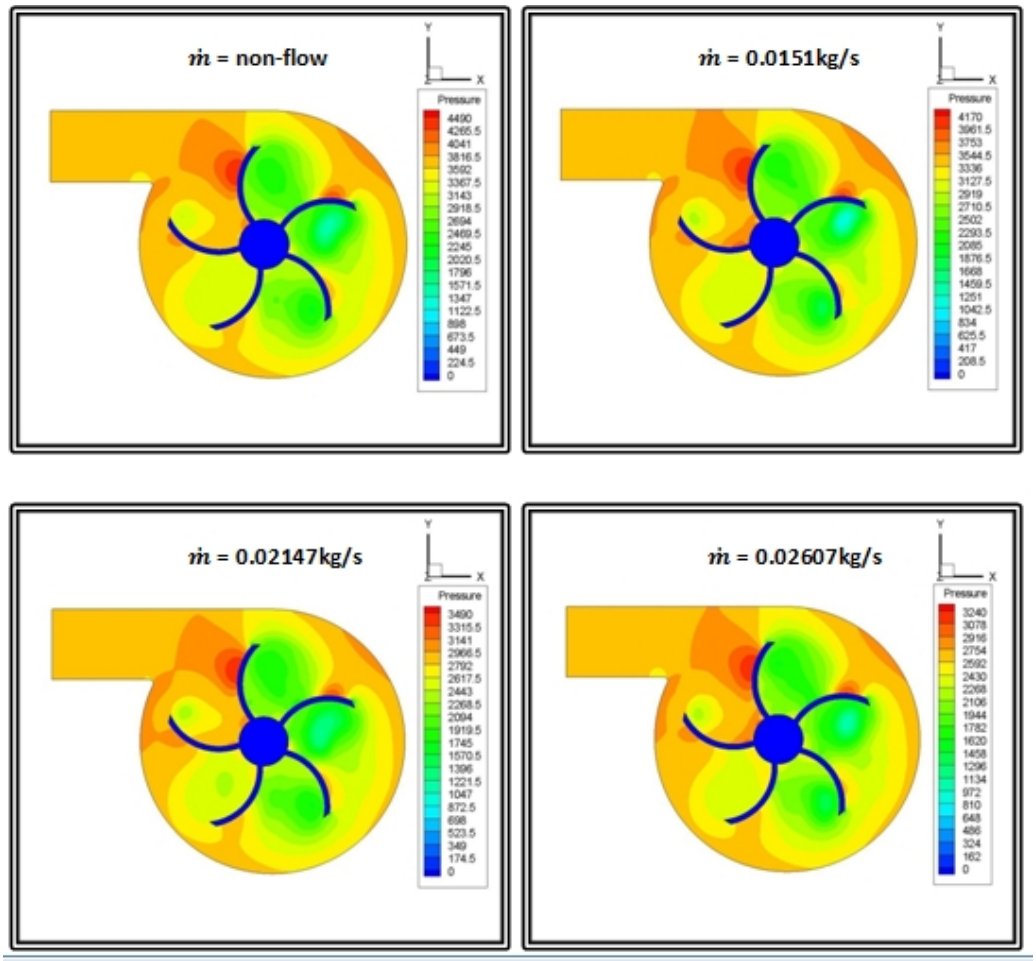

Fig .(15): Contours of Static Pressure for Case (C) at Rotational Speed 16000 rpm.

5. Conclusions

The main task of the present research is to design and construct a research test rig and carry out preliminary experimental tests on it. The static pressures were measured at locations along circumferential paths around the impeller. The results with flow simulation results lead to the following conclusions:

1. The minimum value of static pressure around the impeller for cases (A, C) observed at angular position ($\emptyset = 30^{\circ}$) beyond the tongue at all values of mass flow rates. In case (B) observed the minimum value of static pressure at angular position ($\emptyset = 150^{\circ}$).
2. The maximum pressure drop around the volute observed at angular position ($\emptyset = 120^{\circ}$) and ($\emptyset = 150^{\circ}$) for cases (B, and C).
3. The maximum value of static pressure around the impeller and volute for three cases observed at angular position ($\emptyset = 0^{\circ}$) and ($\emptyset = 330^{\circ}$) for all values of mass flow rates.
4. The pressure fluctuation for various mass flow rates in non-periodical nature, as the mass flow rate is reduced, the pressure fluctuations amplitude increases. The maximum pressure fluctuations amplitude occurs at mass flow rate equal to nearly non-flow.

5. The time and frequency domain analysis indicate that the impeller design for case (B) (with nine number of blades), exhibits high pressure fluctuations comparison with other cases.
6. The rotating stall and pressure drop increase between the impeller passages with decrease number of blade. This due to the increase in vortices and flow separation.
7. Agreement between the numerical and experimental static pressure data in the volute is fairly good; some differences have arisen, especially near the inlet of impeller rejoin.

References

1. **Dixon S. L., ″Fluid Mechanics, Thermodynamics of Turbomachinary″, Fifth Edition, 2005.**
2. **Nicolas Courtiade, ″Experimental Analysis of The Unsteady Flow and Instabilities in a High-Speed Multistage Compressor″, Thesis, 2012.**
3. **Jan T. Gravdahl, ″Modeling and Control of Surge and Rotating Stall in Compressors″, Thesis, Department of Engineering Cybernetics, Norwegian University of Science and Technology, 1998.**
4. **A.S. Hassan "Influence of the volute design parameters on the performance of a centrifugal compressor of an aircraft turbocharger", IMechE, Vol. 221 Part A: J. Power and Energy, 2007.**
5. **Imaiichi. K, and Tsurusaki. H.,"Rotating stall in a vaneless diffuser of centrifugal fan," Flow in Primary, non-Rotating Passage in Turbomachines," The winter annual meeting of the ASME, New York, PP-23-31, 1979.**
6. **M. Hamada S. Tsujita, and T. Sakai, "Flow measurement around a fan volute tongue using particle tracking velocimetry", Proc. Instn Mech Engrs, Vol. 212. Pt A, PP 235-246, 2000.**
7. **Zhou W., Zhao Z., Lee T. S. and Winoto S. H., ″Investigation of Flow Through Centrifugal Pump Impellers Using Computational Fluid Dynamics″, International Journal of Rotating Machinery, Vol.9, PP 49-61, 2003.**
8. **Eduardo B. Marigorta "Fluid-dynamic radial forces at the blade-passing frequency in a centrifugal pump with different impeller diameters", ASME J. Fluid Engineering 124, 401-410, 2006.**
9. **Saad A. Ahmed, "Control of stall in a radial diffuser using rough surfaces", Can, Aeronaut. Space J. , Vol. 54, No. 1, PP. 9-15, 2008.**
10. **Stefan Berten,"Experimental investigation of flow instabilities and rotating stall in a high-energy centrifugal pump stage", Proceedings of ASME Fluids Engineering Division Summer Meeting, FEDSM, 2009.**

11. **Laras Davidson, ″An Introduction to Turbulence Models″, Department of Thermo and Fluid Dynamics, Chalmers University of Technology, Sweden, 2009.**
12. **Versteeg H. K., Malalasekera W., ″An Introduction to Computational Fluid Dynamic, The Finite Volume″, Longman Group Limited, 1995.**
13. **Yonas Teshome, ″CFD Study on The Performance of Regenerative Flow Pump (RFP) with Aerodynamic Blade Geometry″, Thesis, Addis Ababa University, 2007.**
14. **Ahmed A. A., ″Study of Rotating-Stall and Pressure Fluctuation in a Volute of High-Speed Centrifugal Fan″, Thesis, college of engineering, Al-Mustansiriyah University, 2005.**